

# Section 1

## PROGRESS IN LASER FUSION

### 1.A Implicit and Conservative Difference Scheme for the Fokker-Planck Equation

The Fokker-Planck (FP) equation plays an important role in the investigation of electron transport processes in laser-produced plasmas.<sup>1,2</sup> Much of the progress in the numerical solution of the FP equation has been possible following the pioneering work of Chang and Cooper.<sup>3</sup> They proposed a practical differencing scheme that preserved particle number and allowed the distribution function to evolve through a series of quasi-equilibria, while maintaining positivity at all energy groups.

Recently, however, Larsen *et al.*<sup>4</sup> showed that although the Chang-Cooper scheme works well for linear problems, such as the scattering of test particles, it sometimes fails for general nonlinear problems involving the evolution of distribution functions far from equilibrium. Larsen *et al.*<sup>4</sup> generalized the Chang-Cooper method to allow for a more efficient solution of the nonlinear FP equation using larger time steps. Unfortunately, their approach relies on having analytic expressions for the collision coefficients, which are not generally available.

One important property of the FP equation not addressed by the above authors is energy conservation. Langdon<sup>5</sup> introduced this property to the Chang-Cooper scheme, for Coulomb scattering between like particles, by appropriately differencing the collision coefficients. This modification has been successfully tested by Kho<sup>6</sup> and found to ensure adequate energy conservation provided the distribution function does not change substantially over one time step.<sup>2</sup> For modeling thermal-transport problems in laser-produced plasmas, Epperlein *et al.*<sup>1</sup> found that energy conservation could be further improved through a

“predictor” step, whereby the collision coefficients are estimated by linearly extrapolating the distribution function in time. Berezin *et al.*<sup>7</sup> developed further numerical schemes that conserved not only particle energy and density but also maximized entropy. Unfortunately, their methods rely on explicit time integration and are thus of limited practical use.

In this article we develop a fully implicit finite-difference method for solving the FP equation for like-particle collisions in plasma that conserves both energy and number density *exactly*. The essence of our approach is to first linearize the FP equation, with the collision coefficients as defined by Langdon, and then apply the Chang-Cooper approach to difference the equation in velocity space. The conservative properties of the scheme are illustrated by considering the standard test problem<sup>6</sup> of the thermalization of a nearly monoenergetic electron distribution in a homogeneous plasma. It is shown that, whereas the conventional scheme is limited by energy conservation to time steps no larger than about 100 thermal collision times, there is no such limitation with the new scheme.

Although the numerical solution of the finite-difference equation in our proposed scheme requires the inversion of a full matrix rather than a tridiagonal matrix,<sup>3</sup> the relaxation in time-step constraints can sometimes far outweigh the extra computational effort. This is demonstrated by simulating the evolution of a laser-produced plasma using the *SPARK* FP code,<sup>1,2</sup> where we typically gain factors of greater than ten in computational speed.

In the next section the FP equation is described, and its basic conservation properties are reviewed. Then the numerical scheme is developed, and the test problem of electron thermalization in a homogeneous plasma is presented. In the last two sections we describe simulations of laser-produced plasmas using an FP code and summarize the main conclusions.

### The Fokker-Planck Equation and Its Conservation Properties

The FP equation describing Coulomb collisions of like particles in a homogeneous, fully ionized plasma is given by

$$\tau \frac{\partial f}{\partial t} = \frac{v_t^3}{N_0 v^2} \frac{\partial}{\partial v} \left[ C(f) + D(f) \frac{\partial}{\partial v} \right] f \equiv F(f), \quad (1)$$

where  $f(v, t)$  is the normalized particle distribution function, such that

$$N_0 = \int_0^{\infty} dv v^2 f(v, t = 0)$$

is the initial number density. The collision time between thermal particles is defined by

$$\tau = v_t^3 / \left[ 4\pi N_0 (e^2 / m)^2 \ln \Lambda \right],$$

where  $v_t = (T_0 / m)^{1/2}$  is the thermal velocity,  $T_0$  is the initial temperature,  $e$  is the charge,  $m$  is the mass, and  $\ln \Lambda$  is the Coulomb logarithm. The collision coefficients, describing friction and diffusion, are given by<sup>8</sup>

$$C(f) = \int_0^v duu^2 f(u, t) \quad (2)$$

and

$$D(f) = \frac{1}{3v} \int_0^v duu^4 f(u, t) + \frac{v^2}{3} \int_v^\infty duuf(u, t), \quad (3)$$

respectively. The equilibrium solution of Eq. (1) is a Maxwellian,  $f_M = (2/\pi)^{1/2} (N_0/v_i^3) \exp(-v^2/2v_i^2)$ .

Since the particle number density is

$$N(t) = \int_0^\infty dvv^2 f(v, t), \quad (4)$$

we can readily establish its conservation by taking the  $\int_0^\infty dvv^2$  moment of Eq. (1). This gives us

$$\tau \frac{\partial N}{\partial t} = \frac{v_i^3}{N_0} \left[ C(f)f + D(f) \frac{\partial f}{\partial v} \right] \Big|_0^\infty, \quad (5)$$

where the appropriate boundary conditions on  $f$  are that  $[Cf + D(\partial f/\partial v)]$  vanishes at  $v = 0$  and  $\infty$ .

Energy conservation can be verified by taking the  $(1/2)m \int_0^\infty dvv^4$  moment of Eq. (1), i.e.,

$$\tau \frac{\partial E}{\partial t} = \frac{1}{2} m \int_0^\infty dvv^4 F(f) = \frac{1}{2} m \int_0^\infty dvv^4 \left\{ \frac{v_i^3}{N_0 v^2} \frac{\partial}{\partial v} \left[ C(f)f + D(f) \frac{\partial f}{\partial v} \right] \right\}, \quad (6)$$

where  $E [= (3/2)NT]$  is the energy density. Integrating Eq. (6) by parts, and using the fact  $(vDf)$  vanishes at  $v = 0$  and  $\infty$ , we obtain

$$\tau \frac{\partial E}{\partial t} \propto - \int_0^\infty dvv \left( Cf + D \frac{\partial f}{\partial v} \right) = - \int_0^\infty dv \left[ vCf - \frac{\partial(vD)}{\partial v} f \right]. \quad (7)$$

From Eq. (2) and rewriting Eq. (3) as

$$\frac{\partial}{\partial v} (vD) = v^2 \int_v^\infty duuf, \quad (8)$$

we then have

$$\tau \frac{\partial E}{\partial t} \propto - \int_0^{\infty} dv \left[ v C f - \frac{\partial(vD)}{\partial v} f \right] = - \int_0^{\infty} dv v f(v) \int_0^v du u^2 f(u) + \int_0^{\infty} dv v^2 f(v) \int_v^{\infty} du u f(u). \quad (9)$$

By recognizing that the two double integrals on the right-hand side of this equation are identical, we thus have energy conservation.

### The Numerical Scheme

The conventional approach for solving Eq. (1) is to discretize in time such that  $\Delta t = (t^{n+1} - t^n)$  and use  $\partial f / \partial t \approx (f^{n+1} - f^n) / \Delta t$  to obtain<sup>3</sup>

$$\tau \frac{(f^{n+1,i+1} - f^n)}{\Delta t} = \frac{v_i^3}{N_0 v^2} \frac{\partial}{\partial v} \left( C^{n+1,i} f^{n+1,i+1} + D^{n+1,i} \frac{\partial f^{n+1,i+1}}{\partial v} \right), \quad (10)$$

where  $i = 0, \dots, I$  is an iteration index. At the beginning of each iteration, the nonlinear coefficients are then calculated with either  $f^{n+1,i=0} = f^n$  or  $f^{n+1,i=0} = 2f^n - f^{n-1}$  (i.e., a predictor step). However, as will be shown later, such iterative methods can lead to large energy-conservation errors when  $\Delta t \gg \tau$  for plasmas far from thermal equilibrium.

In this article we develop a noniterative, fully implicit method for solving Eq. (1) that conserves energy exactly for arbitrary values of  $\Delta t$ . The first step involves expanding  $F(f)$  by a truncated Taylor series,<sup>9</sup>

$$F^{n+1} = F^n + \left( \frac{\partial F}{\partial f} \right)^n (f^{n+1} - f^n) + O(\Delta t^2). \quad (11)$$

Substituting this equation back into Eq. (1), we then obtain

$$\left[ \frac{\tau}{\Delta t} - \left( \frac{\partial F}{\partial f} \right)^n \right] (f^{n+1} - f^n) = F^n, \quad (12)$$

where

$$\left( \frac{\partial F}{\partial f} \right)^n f^n = 2 F^n$$

and

$$\left( \frac{\partial F}{\partial f} \right)^n f^{n+1} = \frac{v_i^3}{N_0 v^2} \frac{\partial}{\partial v} \left( C^n f^{n+1} + D^n \frac{\partial f^{n+1}}{\partial v} \right) + \frac{v_i^3}{N_0 v^2} \frac{\partial}{\partial v} \left( C^{n+1} f^n + D^{n+1} \frac{\partial f^n}{\partial v} \right). \quad (13)$$

(a)

(b)

Here, we identify terms (a) and (b) as differential and integral operators on  $f^{n+1}$ , respectively. They represent the time rate of change of  $f$  resulting from the distribution of (a) test and (b) field particles at  $t^{n+1}$ . By neglecting the more cumbersome term (b), Eq. (12) reduces to Eq. (10) with  $C^{n+1,i} = C^n$  and  $D^{n+1,i} = D^n$ . However, even though terms (a) and (b) individually conserve number density, we will now show that term (b) is essential to ensure overall energy conservation.

Taking the  $(1/2)m \int_0^\infty dv v^4$  moment of Eq. (12), we find that

$$\frac{\tau}{\Delta t} (E^{n+1} - E^n) - \frac{1}{2} m \int_0^\infty dv v^4 \left( \frac{\partial F}{\partial f} \right)^n (f^{n+1} - f^n) = \frac{1}{2} m \int_0^\infty dv v^4 F^n. \quad (14)$$

Comparing Eq. (14) with Eq. (6) and noting that  $(\partial F / \partial f)^n f^n = 2F^n$  and  $\int_0^\infty dv v^4 F = 0$ , we are left with

$$\frac{\tau}{\Delta t} (E^{n+1} - E^n) = \frac{1}{2} m \int_0^\infty dv v^4 \left( \frac{\partial F}{\partial f} \right)^n f^{n+1}, \quad (15)$$

which can then be expanded (using the techniques described earlier) to

$$\frac{\tau}{\Delta t} (E^{n+1} - E^n) \approx - \int_0^\infty dv v f^{n+1}(v) \int_0^v du u^2 f^n(u) + \int_0^\infty dv v f^n(v) \int_0^v du u^2 f^{n+1}(u) \quad (a) \quad (16)$$

$$- \int_0^\infty dv v f^n(v) \int_0^v du u^2 f^{n+1}(u) + \int_0^\infty dv v f^{n+1}(v) \int_0^v du u^2 f^n(u) = 0. \quad (b)$$

Once again, terms (a) and (b) correspond to the differential and integral operators, as in Eq. (13). These terms cancel each other out and lead to exact energy conservation for arbitrary values of  $f^n$  and  $f^{n+1}$ . We do recall, however, that number-density conservation does not require the use of term (b).<sup>3</sup>

Our remaining task is to difference Eq. (12) in velocity space. We introduce  $f_j = f(v_j)$ , where the index  $j = 1, \dots, J$  denotes a cell center. The cell boundaries are defined by  $v_{j+1/2} = (v_j + v_{j+1})/2$ , where  $v_{1/2} = 0$  and  $v_{J+1/2} = v_{\max}$ , and the cell sizes (not necessarily uniform) are given by  $\Delta v_j = (v_{j+1/2} - v_{j-1/2})$  and  $\Delta v_{j+1/2} = (v_{j+1} - v_j)$ . Equation (12) now becomes (using the convention of summing over repeated indices)

$$\left[ \frac{\tau}{\Delta t} \delta_{jk} - \left( \frac{\partial F}{\partial f} \right)_{jk}^n \right] (f^{n+1} - f^n)_k = F_j^n, \quad (17)$$

where

$$\left(\frac{\partial F}{\partial f}\right)_{jk}^n = \frac{v_l^3}{N_0 v_j^2 \Delta v_j} (A_{jk}^n + B_{jk}^n). \quad (18)$$

The matrix elements, corresponding terms (a) and (b) of Eq. (13) are given, respectively, by

$$\begin{aligned} A_{jk}^n &= -\left(\frac{D_{j-1/2}^n}{\Delta v_{j+1/2}} + \frac{D_{j-1/2}^n}{\Delta v_{j-1/2}}\right) + C_{j+1/2}^n \delta_{j+1/2} - C_{j-1/2}^n (1 - \delta_{j-1/2}), \text{ for } j = k \\ &= \frac{D_{j+1/2}^n}{\Delta v_{j+1/2}} + C_{j+1/2}^n (1 - \delta_{j+1/2}), \text{ for } j+1 = k \\ &= \frac{D_{j-1/2}^n}{\Delta v_{j-1/2}} - C_{j-1/2}^n \delta_{j-1/2}, \text{ for } j-1 = k \\ &= 0, \text{ for } j-1 > k \text{ and } j+1 < k, \end{aligned}$$

and

$$\begin{aligned} B_{jk}^n &= \Delta v_j v_j^2 f_{j+1}^n + (\gamma_{j+1/2}^n - \gamma_{j-1/2}^n) \mu_j S_j, \text{ for } j = k \\ &= \mu_k \left[ \gamma_{j+1/2}^n \Delta v_j v_j^2 + (\gamma_{j+1/2}^n - \gamma_{j-1/2}^n) S_j \right], \text{ for } j < k \\ &= \Delta v_k v_k^2 \left[ f_{j+1/2}^n - f_{j-1/2}^n + (\gamma_{j+1/2}^n - \gamma_{j-1/2}^n) \delta_{k+1/2} v_{k+1/2} \Delta v_{k+1/2} \right] \\ &\quad + \mu_k (\gamma_{j+1/2}^n - \gamma_{j-1/2}^n) S_k, \text{ for } j > k, \end{aligned}$$

with

$$S_j = \sum_{l=1}^{j-1} \Delta v_l v_l^2, \quad \gamma_{j+1/2}^n = \frac{f_{j+1}^n - f_j^n}{v_{j+1/2} \Delta v_{j+1/2}}, \text{ and}$$

$$\mu_j = v_{j+1/2} \Delta v_{j+1/2} \delta_{j+1/2} + v_{j-1/2} \Delta v_{j-1/2} (1 - \delta_{j-1/2}).$$

Following the Chang-Cooper method, we use

$$f_{j+1/2} = (1 - \delta_{j+1/2})f_{j+1} + \delta_{j+1/2}f_j ,$$

where

$$\delta_{j+1/2} = \frac{1}{w_{j+1/2}} - \frac{1}{\exp(w_{j+1/2}) - 1}$$

and  $w_{j+1/2} = \Delta v_{j+1/2} C_{j+1/2} / D_{j+1/2}$ . This type of weighting has been designed to preserve positivity and provide the correct equilibrium solution for  $f$ .<sup>3</sup>

In order to comply with the energy-conservation relations discussed in this article, the collisional terms are calculated from Eqs. (2) and (8) as follows:<sup>5,6</sup>

$$C_{j+1/2} = \sum_{l=1}^j \Delta v_l v_l^2 f_l ,$$

$$(vD)_{j+1/2} = (vD)_{j-1/2} + \Delta v_j v_j^2 \sum_{l=j}^{J-1} \Delta v_{l+1/2} v_{l+1/2} f_{l+1/2} ,$$

and

$$(vD)_{3/2} = \Delta v_1 v_1^2 \sum_{l=1}^{J-1} \Delta v_{l+1/2} v_{l+1/2} f_{l+1/2} .$$

The appropriate boundary conditions give rise to

$$f_{1/2} C_{1/2} + \frac{D_{1/2}}{\Delta v_{1/2}} (f_2 - f_1) = f_{J+1/2} C_{J+1/2} + \frac{D_{J+1/2}}{\Delta v_{J+1/2}} (f_{J+1} - f_J) = 0 ,$$

$$\mu_1 = v_{3/2} \Delta v_{3/2} \delta_{3/2} , \quad \mu_J = v_{J-1/2} \Delta v_{J-1/2} (1 - \delta_{J-1/2}) ,$$

$$\gamma_{J+1/2} = 0 , \quad f_{J+1} = 0 , \quad \text{and} \quad f_{J+1/2} = 0 .$$

### Test Problem

We consider the thermalization of an approximately monoenergetic distribution of particles through small-angle Coulomb scattering. Figure 55.1 shows the typical evolution of such a distribution, obtained by solving Eq. (17). As expected from previous calculations (e.g., Ref. 5), the particles attain close to a Maxwellian distribution  $f_M$  of density  $N_0$  and temperature  $T_0$  in about five collision times.

For the case shown in Fig. 55.1, where the time step was taken to be  $0.1 \tau$ , both iterative and implicit approaches for solving the FP equation are found to be sufficiently accurate. So the question is—What happens to the solution when  $\Delta t \gg \tau$ ?

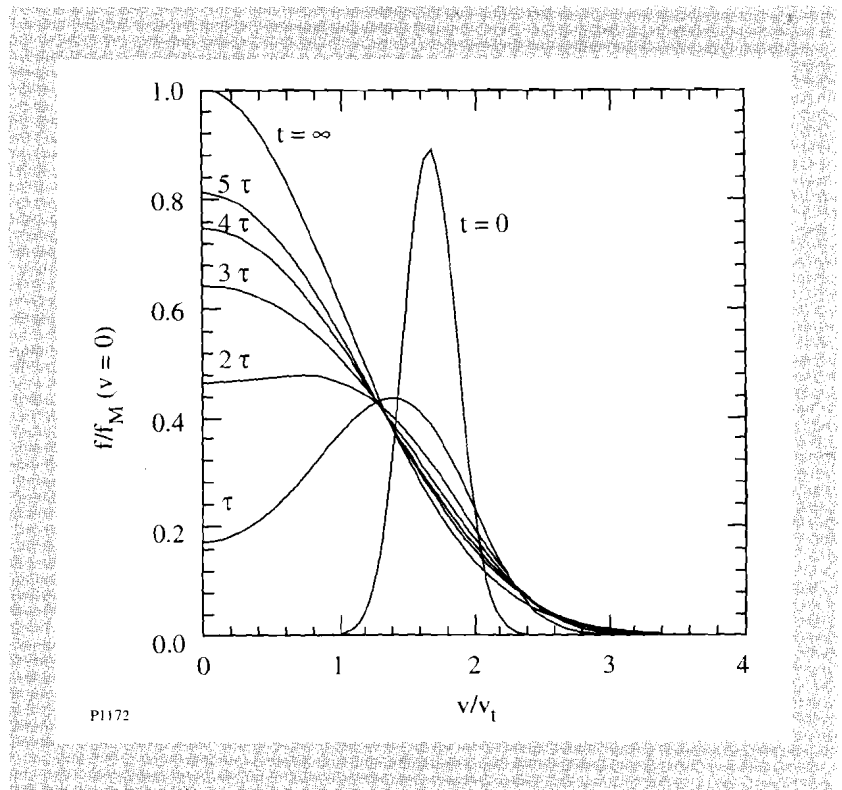


Fig. 55.1  
Plot of the distribution function  $f$  [normalized to  $f_M(v=0)$ ], as a function of velocity  $v$  (normalized to  $v_t$ ), at  $t = 0, \tau, 2\tau, 3\tau, 4\tau, 5\tau$ , and  $\infty$ .

Using the new implicit-conservative scheme we find that the distribution function evolves to the correct Maxwellian steady-state solution in about three time steps, while maintaining constant energy. With the iterative approach, however, the lack of exact energy conservation leads to Maxwellian distribution functions of different temperatures  $T$ . To characterize these results, we calculate the fractional temperature difference  $\left| \frac{T - T_0}{T_0} \right| \equiv \left| \frac{\delta T}{T_0} \right|$  as a function of  $\Delta t/\tau$ . These are plotted in Fig. 55.2, assuming either  $f^{n+1,i=0} = f^n$  or  $f^{n+1,i=0} = 2f^n - f^{n-1}$  (a predictor step). As observed, in the absence of further iterations and for  $\Delta t < 20\tau$ , considerable improvement can be achieved with the predictor step. For  $\Delta t > 20\tau$ , however, neither approach is satisfactory, and the predictor method leads to larger errors. In fact, for  $\Delta t \gg 100\tau$ , the predictor method has been found to produce negative distribution functions and numerical instabilities.

As expected, iterations are found to improve the accuracy of the solutions (see Fig. 55.2). These improvements, however, become less pronounced as  $\Delta t/\tau$  increases, and the energy errors still remain above 20% for  $\Delta t > 100\tau$ , even after ten iterations.

The results presented in Figs. 55.1 and 55.2 are not too sensitive to the initial spread in energy distribution about the most likely energy, though the closer the distribution is to equilibrium, the smaller the energy errors become.

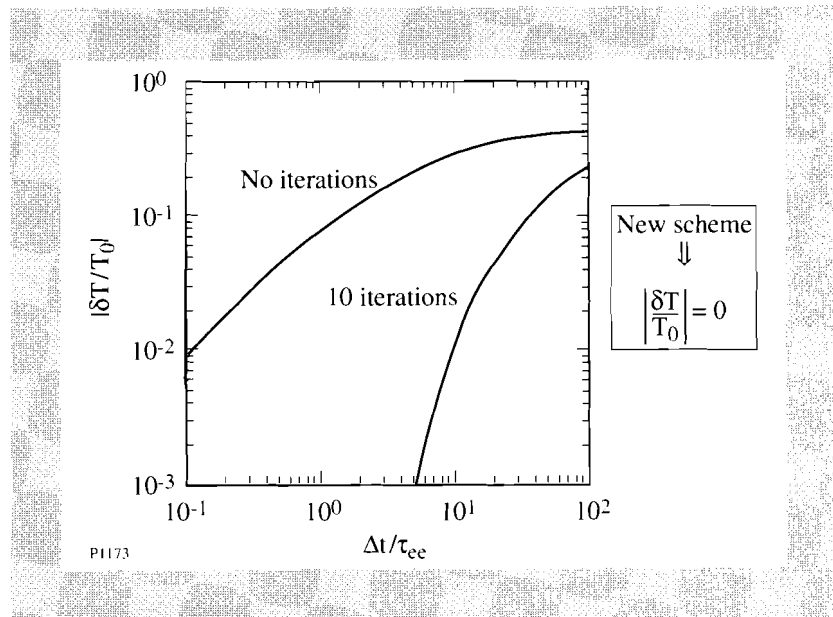


Fig. 55.2

Plot of fractional energy error  $|\delta T/T_0|$ , as a function of  $\Delta t/\tau$ , using either  $f^{n+1,i=0} = f^n$  (solid curves) or  $f^{n+1,i=0} = 2f^n - f^{n-1}$  (dashed curves), and with either no iteration ( $l = 0$ ) or ten iterations ( $l = 10$ ).

### Simulations of Laser-Produced Plasmas

The ablation of a target by a high-power laser, as envisaged in a laser-fusion scenario, has been routinely simulated using the *SPARK* FP code.<sup>1,2</sup> The code assumes fluid ions and solves for the electron-distribution function, including effects such as transport in configuration space, laser heating, and electron thermalization in velocity space. Since the last process is modeled by the same equation considered in this article, its method of solution can have an important impact on the computational efficiency of the code.

As discussed in the previous section, if the time step used in the code is much greater than  $\tau$  (where  $\tau = \tau_{ee}$  is now the thermal collision time between electrons), and the electron-distribution function is far from equilibrium, one might expect significant energy errors when using the standard iterative scheme for the electron-electron collision operator. To demonstrate this effect we simulate the evolution of a laser-produced plasma using *SPARK*.

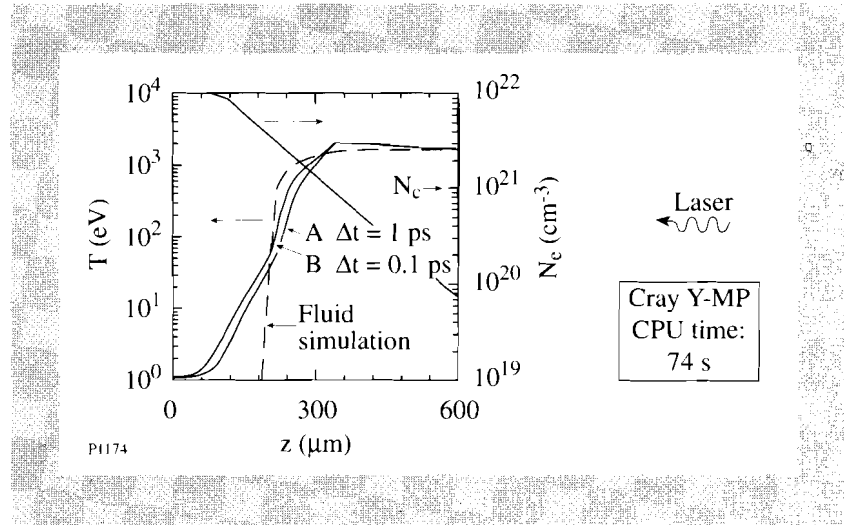
We first consider an idealized planar plasma of the type initially studied by Albritton.<sup>10</sup> The ions are assumed cold, immobile, and fully ionized, with an effective ionization number of  $Z = 10$ . Figure 55.3 shows the corresponding electron-number-density profile as a function of space  $z$ . A 1.06- $\mu\text{m}$  laser is incident from the right, with its energy being deposited via inverse-bremsstrahlung (up to the critical density,  $N_0 = N_c = 10^{21} \text{ cm}^{-3}$ ) at a constant intensity of  $10^{14} \text{ W/cm}^2$  over a period of 100 ps. Unlike Albritton, however, we assume a much lower initial electron temperature of 1 eV.

*SPARK* is run with 40 zones in  $z$  and 40 feathered zones in  $v$ , such that  $\Delta v_{j+1} / \Delta v_j = 1.11$  and  $v_{\text{max}} = 200 v_r$ . Using the implicit-conservative scheme we find that a constant time step of 0.1 ps provides a converged solution for the thermal heat front (shown in Fig. 55.3). The overall CPU time for this simulation is 74 s on a Cray Y-MP. To highlight the nonlocal nature of the electron transport, Fig. 55.3 also plots the temperature profile (dashed curve) based on a fluid description of the energy equation, using the Spitzer-Härm heat flow formula.<sup>11</sup>

This shows certain well-known features of nonlocal transport,<sup>10,1</sup> such as inhibition of the main heat front and preheat due to long-mean-free-path electrons coming from the corona.

Fig. 55.3

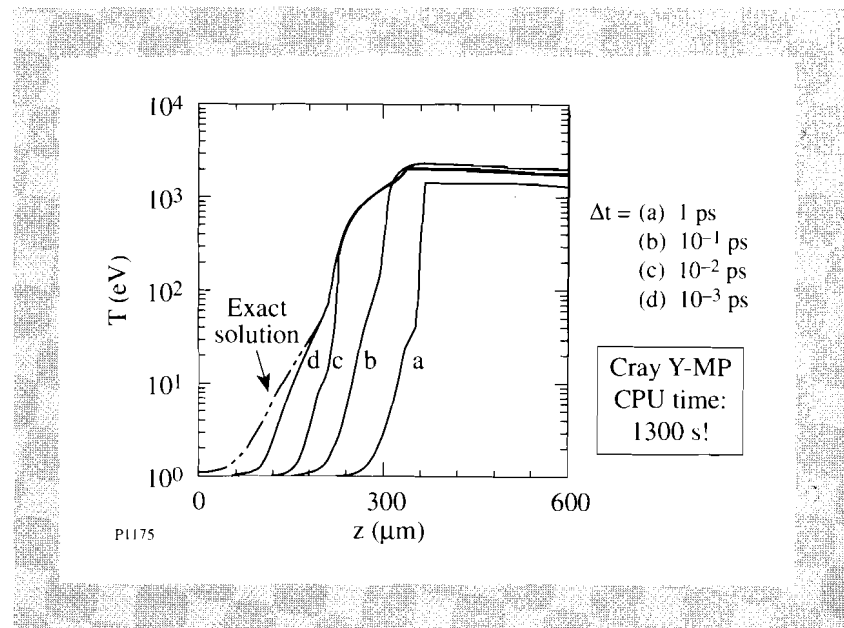
Plots of electron number density  $N$  (in  $\text{cm}^{-3}$ ) and temperature  $T$  (in eV), as functions of  $z$  (in  $\mu\text{m}$ ). Solid curves are obtained using the implicit-conservative scheme on SPARK, with (a)  $\Delta t = 1$  ps and (b)  $\Delta t = 0.1$  ps, and dashed curves are based on fluid model results. The critical density is identified by  $N_c$ .



The above simulations have been repeated using the conventional iterative method for the electron-electron collision operator. Figure 55.4 plots the resulting temperature profiles for  $\Delta t = 1, 10^{-1}, 10^{-2},$  and  $10^{-3}$  ps, assuming  $f^{n+1,i=0} = f^n$  (followed by one iteration). The corresponding CPU times are 1.3, 13, 130, and 1300 s. A comparison between Figs. 55.3 and 55.4 shows the slow convergence of the iterative scheme. This is specially true at high densities, where the preheat is occurring. Also, even though curve  $d$  (in Fig. 55.4) is not yet fully converged, it has already taken 18 times more computational effort than the corresponding curve  $b$  (in Fig. 55.3). The predictor scheme, which assumes that  $f^{n+1,i=0} = 2f^n - f^{n-1}$  (followed by one iteration), turns out to be impractical in this case since it leads to numerical instability for  $\Delta t > 10^{-3}$  ps.

Fig. 55.4

Plots of electron temperature  $T$  (in eV) as a function of  $z$  (in  $\mu\text{m}$ ). Results are based on the iterative scheme with one iteration and (a)  $\Delta t = 1$  ps, (b)  $\Delta t = 10^{-1}$  ps, (c)  $\Delta t = 10^{-2}$  ps, and (d)  $\Delta t = 10^{-3}$  ps (same conditions as in Fig. 55.3).



To understand the poor performance of the iterative scheme we must first realize that the electron-distribution function is far from a Maxwellian. This is shown in Fig. 55.5, which plots  $f$  as a function of electron kinetic energy  $(1/2)mv^2$  (in keV), corresponding to positions (A) and (B) in Fig. 55.3. Here we note the typical<sup>10</sup> double-Maxwellian nature of the electron distribution in the overdense region (A), where the “hot” tail shares the same temperature as the tail of the distribution at the critical density (B). Another important clue to the poor performance of the iterative scheme lies in the values of  $\tau_{ee}$ , which are plotted in Fig. 55.6 (for the same conditions as in Fig. 55.3). Together with the discussion in the “test problem” section, this figure shows why the convergence of the iterative scheme is so slow at high densities and low temperatures. Indeed, even for  $\Delta t = 10^{-3}$  ps, the high-density unheated plasma has a characteristic  $\tau_{ee} \sim 0.01 \Delta t$ .

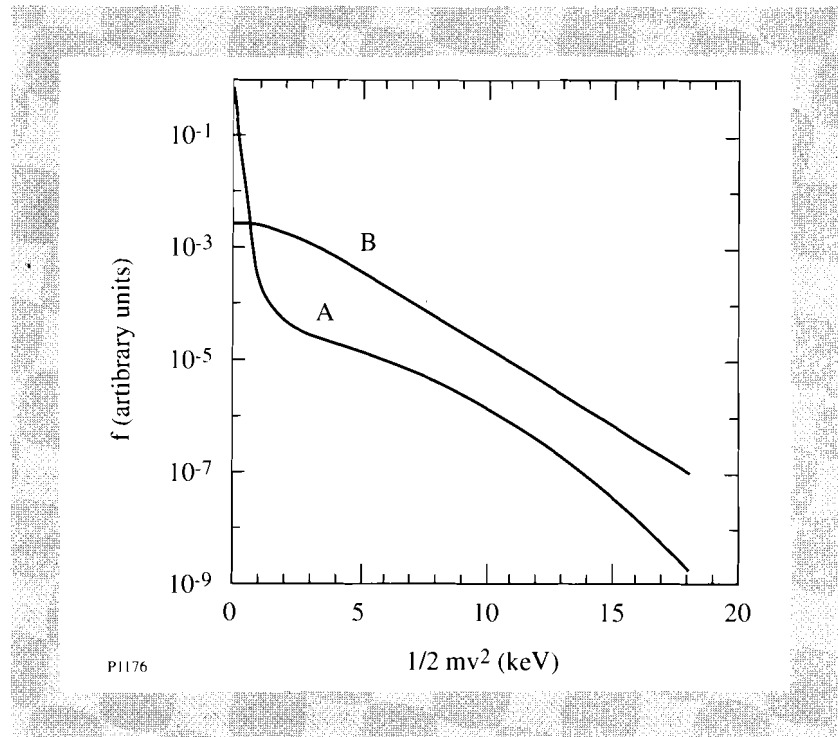


Fig. 55.5  
Plots of  $f$  (in arbitrary units) as a function of electron kinetic energy  $(1/2)mv^2$  (in keV). Curves correspond to positions A and B in Fig. 55.3.

To test the implicit-conservative scheme under less-idealized plasma conditions, we now consider the recent Rayleigh-Taylor experiments performed at Lawrence Livermore National Laboratories using the NOVA laser.<sup>12</sup> We attempt to model their plasma conditions by simulating the evolution of a CH foil, illuminated by 530-nm laser light with 1-ns linear rise time followed by a 2-ns flat section, at an intensity of  $5 \times 10^{13}$  W/cm<sup>2</sup>.

Our initial conditions correspond to a fully ionized, 18-mm CH plasma at a temperature of 0.5 eV and an electron number density of  $3.38 \times 10^{23}$  cm<sup>-3</sup>. The code is run in one-dimensional planar geometry on a Lagrangian mesh, assuming cold fluid ions. The configuration space mesh uses 50 zones, and the velocity mesh uses 35 feathered zones (where the mesh size increases at a constant ratio,  $\Delta v_{j+1} / \Delta v_j = 1.11$ ) and  $v_{\max} = 280 v_I$ .

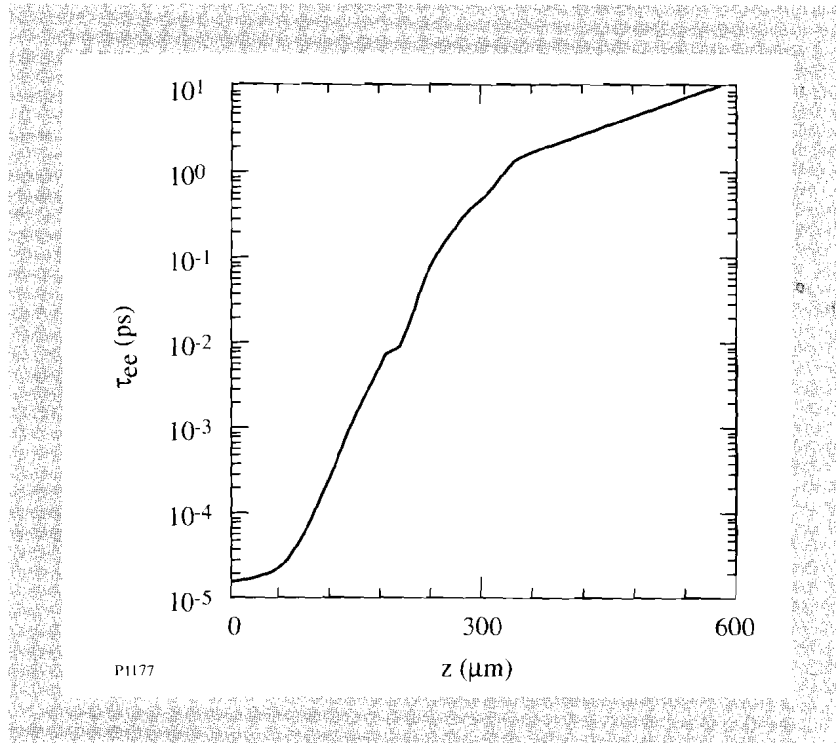


Fig. 55.6

Plot of  $\tau_{ee}$  (in picoseconds) as a function of  $z$  (in microns) (same conditions as in Fig. 55.3).

Figure 55.7 plots the electron temperature and number density as functions of space  $z$  at 3 ns. The implicit-conservative scheme has been used with a constant time step of 1 ps. The overall computation time of the simulation is 230 CPU sec on a Cray Y-MP.

In this case, to obtain a similarly accurate solution, the conventional iterative scheme (with one iteration) would require a prohibitively small time step of  $<10^{-5}$  ps. By using the predictor step (followed by one iteration), however, it has been possible to successfully reproduce the results in Fig. 55.7 with  $\Delta t = 0.01$  ps. (Unfortunately, this type of iterative scheme leads to numerical instabilities for  $\Delta t > 0.01$  ps.) This uses a total of 7200 CPU sec of computational time. So despite the fact that the implicit-conservative scheme requires three times more computational effort per  $\Delta t$ , the 100-fold increase in  $\Delta t$  has produced a 30-fold enhancement in computational speed.

It must be realized that many factors can affect the relative efficiency of using the implicit-conservative scheme. An obvious one is the value of  $\tau_{ee}$ , as demonstrated by the previous numerical simulations; another is the number of velocity groups  $J$ . Since the solution of Eq. (17) requires inversion of a full matrix rather than a tridiagonal matrix [as required by Eq. (10)], the computational effort scales approximately as  $J^2$  instead of  $J$ . This explains the larger computational effort (per time step) required by the implicit-conservative scheme. Although this can eventually limit the size of  $J$ , it is found that in practice one can alleviate this problem by judiciously feathering the velocity mesh (as done in the above simulations).

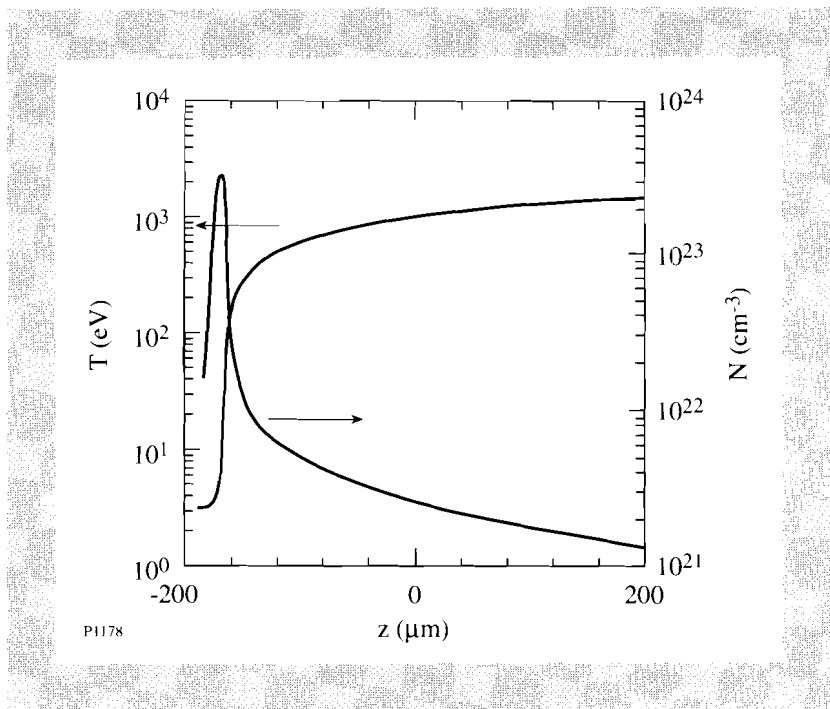


Fig. 55.7

Plots of electron number density  $N$  (in  $\text{cm}^{-3}$ ) and temperature  $T$  (in eV), as a function of  $z$  (relative to initial target position in microns), at  $t = 0$  and 3 ns. Results are obtained using the implicit-conservative scheme on *SPARK* with  $\Delta t = 1$  ps.

### Conclusions

In this article an implicit finite-difference scheme has been developed for solving the FP equation for like-particle collisions in plasmas. Unlike the currently available schemes, it enforces not only number-density conservation, but also exact-energy conservation. These properties have been demonstrated both analytically and numerically by considering the thermalization of an approximately monoenergetic distribution of particles. It is shown that even when the numerical integration time step is much larger than the thermal collision time, the correct steady-state solution is obtained. By comparison, numerical solutions based on conventional iterative approaches can yield unacceptably large energy errors.

The usefulness of the new implicit-conservative scheme has been demonstrated by implementing it in the laser-plasma transport code *SPARK*. Apart from improving the reliability of the code, the relaxation in time-step constraints has typically allowed for over an order of magnitude reduction in computational time.

### ACKNOWLEDGMENT

I wish to thank Dr. R. W. Short for many helpful discussions. This work was supported by the U.S. Department of Energy Office of Inertial Confinement Fusion under Cooperative Agreement No. DE-FC03-92SF19460, the University of Rochester, and the New York State Energy Research and Development Authority. The support of DOE does not constitute an endorsement by DOE of the views expressed in this article.